Palaeomagnetic and anisotropy of magnetic susceptibility data bearing on the emplacement of the Western Granite, Isle of Rum, NW Scotland

M. S. PETRONIS*†, B. O'DRISCOLL‡§, V. R. TROLL‡, C. H. EMELEUS¶ &
J. W. GEISSMAN*

*Department of Earth and Planetary Sciences, University of New Mexico, Albuquerque, NM 87131, USA
‡Department of Geology, Museum Building, Trinity College, Dublin 2, Ireland
¶Department of Earth Sciences, University of Durham, Science Laboratories, South Road, Durham, DHI 3 LE, UK

Abstract – The Western Granite is the largest of several granitic bodies around the margin of the Rum Central Igneous Complex. We report palaeomagnetic and anisotropy of magnetic susceptibility (AMS) data that bear on the emplacement and deformation of the Western Granite. The collection includes samples from 27 sites throughout the Western Granite, five sites in adjacent feldspathic peridotite, and two sites in intermediate to mafic hybrid contact aureole rocks. Palaeomagnetic data from 22 of the 27 sites in the granite provide an *in situ* group mean D = 213.2°, I = −69.5°, α_{95} = 5.5° that is discordant to an early Paleocene reverse polarity expected field (about 184°, −66°, α_{95} = 4.3°). The discrepancy is eliminated by removing an inferred 15° of northwest-side-down tilting about a best fit horizontal tilt axis trending 040°. Data from the younger peridotite and hybrid rocks of the Rum Layered Suite provide an *in situ* group mean of D = 182.6°, I = −64.8°, α_{95} = 4.0°, which is statistically indistinguishable from an early Paleocene expected field, and imply no post-emplacement tilting of these rocks since remanence acquisition. The inferred tilt recorded in the Western Granite, which did not affect the younger Layered Suite, suggests that emplacement of the ultrabasic rocks resulted in roof uplift and associated tilt of the Western Granite to make space for mafic magma emplacement. Magnetic fabric magnitude and susceptibility parameters yield two subtle groupings in the Western Granite AMS data set. Group 1 data, defined by rocks from exposures to the east and south, have comparatively high bulk susceptibilities (K_{mean}, 29.51 × 10^{-3} in SI system), stronger anisotropies (P_j, 1.031) and oblate susceptibility ellipsoids. Group 2 data, from rocks in the west part of the pluton, have lower values of K_{mean} (15.89 × 10^{-3} SI) and P_j (1.014), and triaxial susceptibility ellipsoids. Magnetic lineations argue for emplacement of the granite as a tabular sheet from the south–southeast toward the north and west. Moderate to steeply outward-dipping magnetic foliations, together with deflection of the country rock bedding in the north, are consistent with doming accompanying magma emplacement.

Keywords: palaeomagnetism, anisotropy of magnetic susceptibility, magma emplacement, Isle of Rum, granite.

1. Introduction

The British Palaeogene Igneous Province (BPIP) has been a key area for the study of igneous processes for well over a century (e.g. Judd, 1889; Geikie, 1897; Harker, 1904, 1908; Bailey *et al.* 1924; Richey & Thomas, 1930; Richey, 1932), and research on the province has contributed to our understanding of subvolcanic magma transport and emplacement processes. This region has also been noted for its diverse assemblage of magma types, particularly the common occurrence of mixed mafic and felsic compositions (Blake *et al.* 1965; Gamble, 1979; Sparks, 1988; Troll, Donaldson & Emeleus, 2004). In this respect, the origin and emplacement of felsic magma bodies has been of great interest (Walker, 1975; Meighan, 1979;

Thompson, 1982; England, 1992; Gamble, Meighan & McCormick, 1992; Meighan, Fallick & Mccormick, 1992; McCormick *et al.* 1993; Stevenson *et al.* 2007), and no universally accepted model presently exists to explain their genesis. The Western Granite on the Isle of Rum (Inner Hebrides, NW Scotland) is the largest of several granitoid bodies around the margin of the Rum Igneous Centre, all of which are interpreted as part of the early felsic updoming and caldera collapse stage (Stage 1) that preceded the intrusion of the Rum Layered Suite (Stage 2; Emeleus *et al.* 1996; Emeleus, 1997).

The origin and emplacement history of the Western Granite is obscured by the paucity of primary intrusive contacts with the country rocks and lack of macroscopic igneous fabrics. Initial work suggested that the Western Granite originated through metasomatic alteration of feldspathic sandstones of the Proterozoic Torridonian Group (Black, 1952, 1954). Subsequent investigation demonstrated that Black's proposed continuous transition from sandstone to microgranite does

†Author for correspondence: mspetro@nmhu.edu; now at Environmental Geology, Natural Resource Management Department, New Mexico Highlands University, P.O. Box 9000, Las Vegas, NM 87701, USA
§School of Physical and Geographical Sciences, Keele University, Keele ST5 5BG, UK
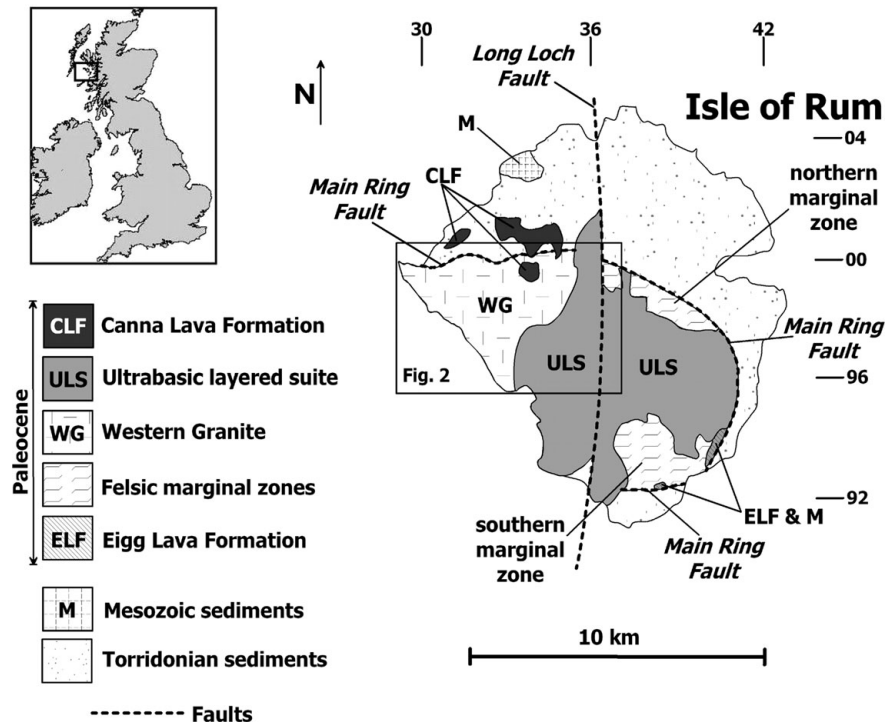
Figure 1. Simplified geological map of the Isle of Rum depicting the major geological units and structural features after Emeleus (1997). Coordinates in UK National Grid (NM and NG).
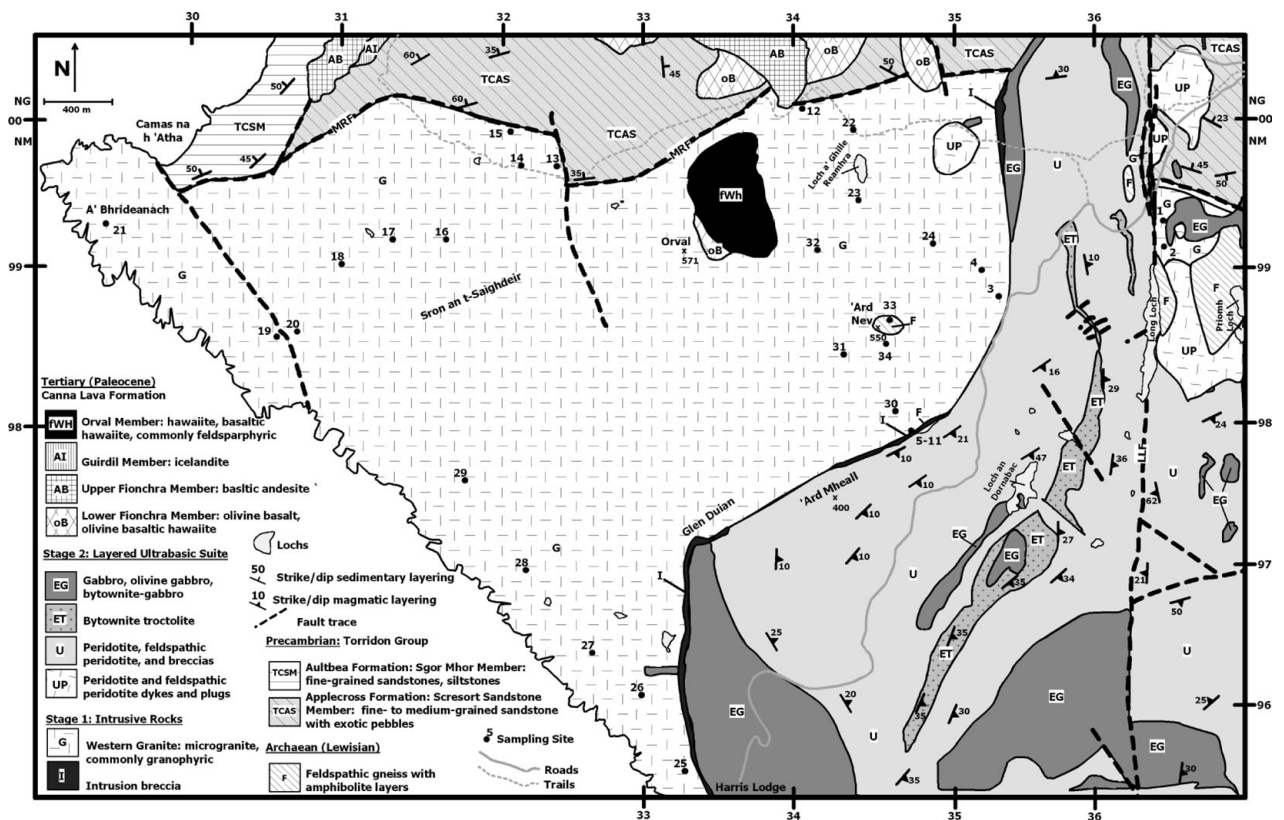

Figure 2. Simplified geological map of the Western Granite and surrounding area. LLF – Long Loch Fault; MRF – Main Ring Fault. Coordinates in UK National Grid. Modified from Emeleus (1994).

not exist (Hughes, Wadsworth & Emeleus, 1957) and that these rocks were juxtaposed by a fault, the effects of which had been heavily overprinted by a later, cross-cutting intrusion of feldspathic peridotite. To the north, the Western Granite is truncated by a vertical to steeply

south-dipping fault system, generally envisioned as the westward continuation of the Main Ring Fault that bounds much of the Central Complex in the east and south of Rum (Emeleus, 1997) (Figs 1, 2). The western edge of the Western Granite, in turn,

is defined by sea cliffs, whereas to the south and southeast it is intruded by ultrabasic intrusive rocks of Stage 2 and marked by extensive intrusion breccias and hybridization. The sole remnants of original Western Granite contacts with the country rock crop out on the summit and southern flank of Ard Nev (N57.02, W6.37; Fig. 2), where a presumed roof pendant of Archaean Lewisian gneiss is intruded by the granite. Apart from this, information on the age and emplacement history of the Western Granite is provided by a single $^{40}Ar-^{39}Ar$ age spectrum determination on biotite of 60.01 ± 0.45 Ma (Chambers, Pringle & Parrish, 2005), apparent geochemical similarities to the rhyodacites and other rocks belonging to Stage 1 (Dunham, 1968; Donaldson, Troll & Emeleus, 2001), and the cross-cutting contacts of the younger Layered Suite.

To understand the emplacement history and the intrusive geometry of the Western Granite, we carried out a combined petrographic, palaeomagnetic and AMS (anisotropy of magnetic susceptibility) study of the Western Granite. Considerable petrological variation within the pluton is shown at the hand sample and thin-section scale, suggesting that the body may in fact represent multiple intrusions. Modest, post-emplacement wholescale gentle tilting of the pluton in the late Palaeogene is inferred from discordant palaeomagnetic data from the granite and is most likely the result of emplacement of the Layered Suite. One preferred interpretation of the AMS data suggests that the intrusion has an overall dome-like geometry in map view, and its major feeder zone may lie to the south–southeast of the granite mass in the central part of the island (Fig. 1). We hypothesize that granite emplacement resulted in a domal geometry to the intrusion and that the AMS and palaeomagnetic data reflect this emplacement style.

2. Geological setting

The Palaeogene Isle of Rum igneous centre developed in two separate stages. During Stage 1, central uplift on a major arcuate fault system, the Main Ring Fault (Bailey, 1945), was accompanied by felsic and mixed felsic/mafic magmatism and the formation of a caldera which filled with felsic ash flows, tuffs and breccias (Emeleus, 1997; Troll, Emeleus & Donaldson, 2000). The country rocks are domed over the central complex, while uplift along the ring faults brought masses of Lewisian gneiss and basal members of the Torridon Group to the present structural levels. Subsequent caldera subsidence resulted in the preservation of Jurassic sedimentary rocks and Paleocene basaltic lavas of the Eigg Lava Formation in the Main Ring Fault (Fig. 1). Shortly after this movement on the Main Ring Fault, several microgranites were intruded, including the Papadil and Long Loch bodies, as well as the more extensive Western Granite (Fig. 2). Further uplift probably occurred on the Main Ring Fault system following emplacement of the Western Granite.

During the original geological survey of Rum (Harker, 1908), many exposures were identified in which the peridotites, troctolites and gabbros in the Central Intrusion of the Layered Suite had been intruded by microgranite and porphyritic rhyodacite, from which it was concluded that the felsic rocks were the younger. Wherever the mafic rocks are in contact with felsic rocks, there are spectacular breccias in which angular to sub-rounded mafic rocks are embedded in a network of veins and dykes of fine- to medium-grained microgranite. This interpretation was later challenged, and it is now thought that the breccias are intrusion breccias, formed when hot mafic magmas chilled against, but also melted or partially melted and remobilized, silicic country rocks. These were principally microgranite and porphyritic rhyodacite, but also sandstones and feldspathic gneisses (Hughes, Wadsworth & Emeleus, 1957; Hughes, 1960; Dunham, 1968; Emeleus, 1997). The relatively low-temperature, rheomorphic silicic melts burst through and fragmented the chilled and contracting margins of the mafic intrusions, locally producing sinuous, rounded liquid–liquid contacts where still-liquid mafic magma chilled against the relatively low-temperature felsic liquids, while in some instances, hybrid rocks were formed when heated felsic magma was able to mingle with mafic magma (Emeleus & Troll, in press). Thus, it is now generally accepted that the rocks of the Layered Suite post-date the felsic rocks (Western Granite) of Rum.

Stage 2 commenced with the intrusion of a suite of basaltic cone-sheets and numerous basaltic dykes, many of which trend NW–NNW, followed by emplacement of the Rum Layered Suite (feldspathic peridotites, troctolites and gabbros). In eastern Rum, the mafic and ultramafic rocks form prominent, gently dipping macro-rhythmic layers (generally termed 'Units') some tens of metres in thickness, and make up the Eastern Layered Intrusion. Layered rocks also crop out in SW Rum where they form the Western Layered Intrusion, bordering and intruding the Western Granite (Fig. 1). The Eastern and Western Layered Intrusions are separated by the Central Intrusion, which is composed of a N–S belt of igneous breccias composed of blocks and megablocks of feldspathic peridotite and (commonly layered) troctolites enclosed in matrices of similar lithologies. The Central Intrusion is regarded as representing the feeder system for the Layered Suite and is located along a major N–S fracture, the Long Loch Fault (Emeleus *et al.* 1996; Emeleus, 1997; O'Driscoll *et al.* 2007) (Fig. 1).

3. Petrography of the Western Granite

3.a. Silicate mineralogy

Samples of the Western Granite collected for AMS and palaeomagnetic analysis are largely granophyric microgranite, dominated by quartz, K-feldspar and sodic plagioclase (combined quantities of up to 85 %) (Fig. 3). Considerable textural variation is observed in the granite at the outcrop scale, and abrupt grain
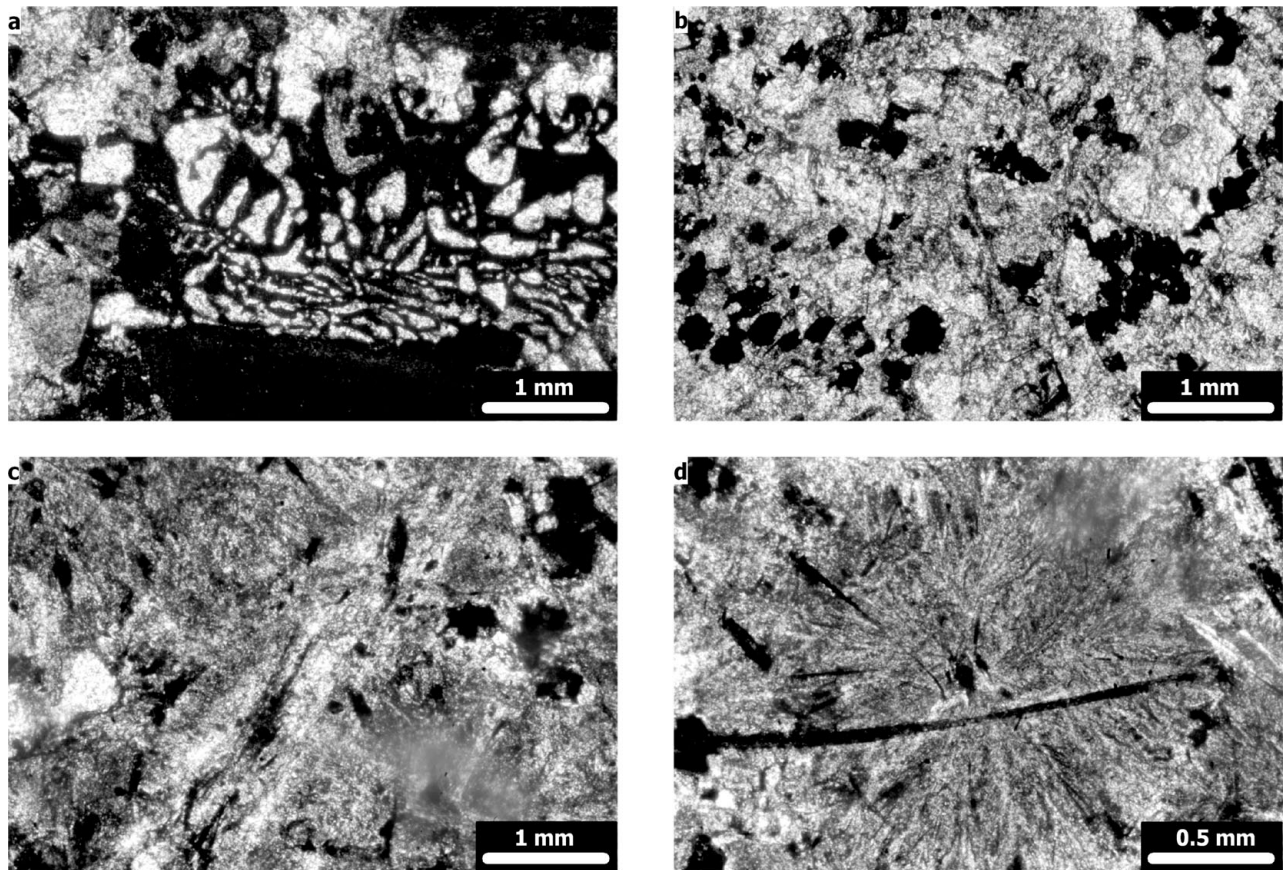
Figure 3. Representative thin-section photomicrographs of rock textures from the Western Granite.

size variation is common, as are frequent irregularly distributed concentrations of drusy cavities, which contain quartz and calcite (Emeleus, 1997). Most quartz and K-feldspar in the rock form radiate graphic intergrowths around plagioclase grains, a feature observed in many samples examined in this study (Fig. 3). Both feldspars usually exhibit turbid grain surfaces, and partial alteration to aggregates of fine-grained white mica is common. This effect is much more pronounced in the western part of the intrusion, while samples collected from the eastern part of the Western Granite are relatively fresh and do not display heavy alteration. Mafic phases are principally biotite and hornblende and make up less than 10 modal %. Interstices are filled in with apatite and chlorite, and opaque grains are also observed. Clinopyroxene is often altered, though Emeleus, Dunham & Thompson (1971) note the presence of relatively fresh ferropigeonite and ferroaugite in the NE part of the intrusion. A facies containing fayalite occurs in the southern part of the intrusion; this also contained green ferrohedenbergite (Emeleus, 1997). Importantly, no evidence of a fabric, magmatic or solid-state, is observed in the field or in thin-section.

3.b. Oxide mineralogy

Oxide minerals in the Western Granite have distributions of opaque grains that are somewhat typical of many felsic to intermediate intrusions (that is, subequant grains (50–100 μm in size)), and these occur predominantly as interstitial material in the granite silicate framework in volume concentrations of 0.5–2 % (Fig. 4). The opaque grains are typically Fe–Ti oxides, and are often associated spatially with biotite and hornblende crystals (Figs 3, 4). This observation is supported by the study of Black (1954), who noted the presence of minor magnetite 'phenocrysts' (frequently associated with hornblende) as equidimensional grains and as long slender rods up to 100 μm in size. Emeleus (1997) also notes the presence of magnetite grains in the granite groundmass. Our observation that biotite is frequently intimately intergrown with Fe–Ti oxides is similar to that of Stevenson, Owens & Hutton (2007).

Back-scattered electron images, obtained using a JEOL 8200 electron Microprobe at the University of New Mexico, of selected areas in polished thin-sections of samples WG3 and WG12 reveal the following observations. Based on petrographic inspection and energy dispersive X-ray analysis, Fe–Ti oxides bright in BSE images (Fig. 4) include an abundance of hemo-ilmenite, ilmeno-hematite and magnetite. The distribution of these phases is highly irregular, with volumes in these rocks containing locally very high concentrations of oxides (Fig. 4). Other volumes are characterized by irregular distributions of exclusively fine, less than 10 μm, oxide grains localized along silicate grain boundaries. Many relatively coarse
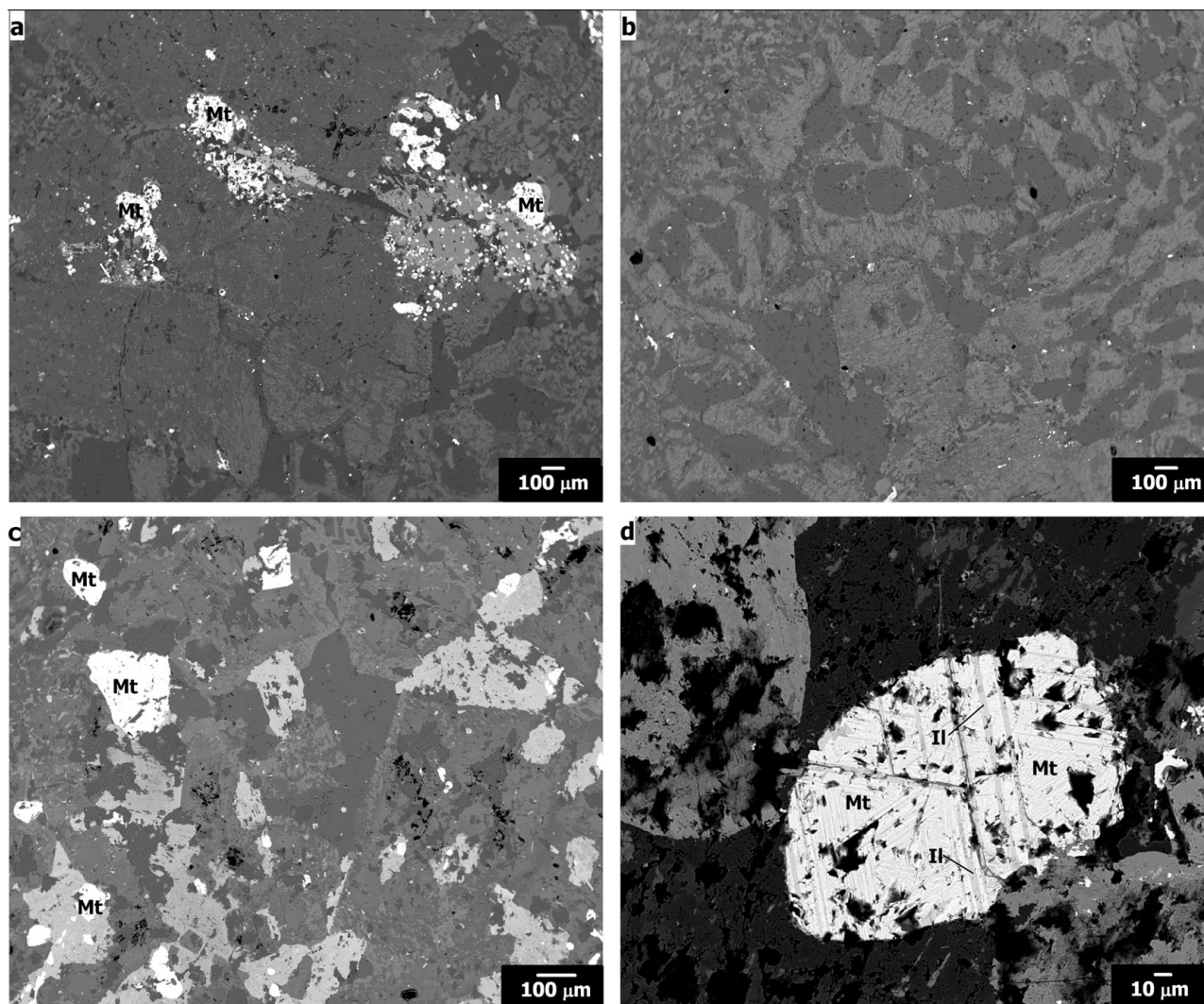
Figure 4. Representative back-scattered electron photomicrographs of oxide mineral textures. Bright, high atomic number phases are Fe–Ti oxides. Mt – magnetite; Il – ilminite.

magnetite grains show evidence of high-temperature oxidation exsolution and the formation of abundant ilmenite lamellae (Fig. 4).

4. Analytical methods

4.a. Sampling technique

Samples were collected as oriented drill-cores from 27 sites throughout the Western Granite using a portable drill with a non-magnetic diamond bit. Five sites in feldspathic peridotite, two sites in intermediate to mafic hybrid rocks in a contact traverse close to Ard Mheall, and one site in Lewisian gneiss close to the summit of Ard Nev, were also established (Fig. 2). All samples were oriented using a magnetic and, when possible, a sun compass. We confined sampling to elevations between 200 m and 500 m (350 ± 150 m) of the exposed intrusion. At each site, from six to 14 independent samples (typically eight) were drilled over an area of about 25 m^2. Core samples were cut into 2.2 by 2.5 cm right cylinder specimens, using a

diamond-tipped, non-magnetic saw blade with up to three specimens per sample obtained.

4.b. Palaeomagnetism

Remanent magnetizations of all samples were measured using a three-axis 2-G Enterprises Model 760R magnetometer at the University of New Mexico with an integrated alternating field (AF) demagnetizing unit. Specimens were progressively AF demagnetized, typically in 15 to 20 steps to a maximum field of 120 mT. Samples with high coercivity were treated with thermal demagnetization up to a maximum of 630 °C, with most samples being fully demagnetized by 580 °C. Thermal demagnetization on replicate specimens, to compare with AF behaviour, was conducted with a Schonstedt TSD-1 thermal demagnetizer. Principal component analysis (PCA; Kirschvink, 1980) was used to determine the best-fit line through selected demagnetization data points for each sample (Table 1). For most samples, a single best-fit line could be fit to the demagnetization data points. Best-fit magnetization

Table 1. Palaeomagnetic data: Isle of Rum, NW Scotland

Site	Unit	n/N	R	in situ Dec	in situ Inc	α_{95}	k	VGP (in situ) Lat	VGP (in situ) Long
				Western Granite					
WG1*	WGS	7/7	6.90	176.9	−44.4	9.2	37.82	59.0	179.1
WG2	WGS	6/9	5.90	212.0	−50.7	7.0	78.36	56.2	119.3
WG3	WG	4/6	3.90	243.3	−73.5	15.7	26.43	57.8	52.4
WG4	WG	5/7	4.80	210.9	−67.8	19.3	13.40	70.9	89.5
WG11	WG	5/6	4.90	187.0	−70.7	2.3	913.95	85.6	108.2
WG12	WG	10/10	9.94	157.1	−61.6	4.1	141.63	69.7	229.0
WG13	WG	8/9	7.90	226.8	−79.6	3.2	267.89	66.3	32.4
WG14	WG	4/6	3.90	272.4	−67.6	3.5	514.97	39.3	48.4
WG15	WG	9/9	8.89	236.9	−66.5	6.1	71.72	55.9	72.4
WG16	WG	9/9	8.96	231.3	−67.8	3.6	202.38	59.9	73.3
WG17	WG	8/8	7.98	226.8	−65.1	2.9	360.54	60.3	82.7
WG18	WG	9/9	8.98	236.3	−71.8	2.9	327.63	60.1	60.1
WG19	WG	4/7	3.97	205.1	−64.1	8.5	118.07	70.9	108.8
WG20*	WG	5/5	4.90	6.3	−73.4	11.5	36.38	26.3	350.1
WG21	WG	7/9	6.76	67.4	58.6	12.2	25.27	43.9	76.1
WG22	WG	9/9	8.94	205.7	−73.7	4.6	124.33	76.3	61.7
WG23	WG	7/8	6.95	281.4	−75.7	5.2	118.40	44.3	32.2
WG24*	WG	9/9	8.95	119.8	−68.6	3.9	172.19	55.8	281.5
WG25	WG	6/7	5.90	172.3	−64.4	6.7	85.36	78.2	200.7
WG26	WG	8/9	7.90	174.3	−52.9	7.9	43.80	66.1	185.5
WG27	WG	9/9	8.97	229.8	−71.2	3.4	229.03	63.0	65.0
WG28	WG	6/8	5.95	211.6	−56.8	6.9	94.93	61.4	113.4
WG29*	WG	8/8	7.97	287.0	−53.3	3.6	238.73	20.0	51.1
WG30	WG	9/9	8.85	201.7	−58.6	7.2	51.86	67.3	125.7
WG31#	WG								
WG32	WG	8/9	7.98	231.8	−80.2	2.6	464.12	64.5	30.3
WG34	WG	6/6	5.98	176.3	−67.9	3.9	236.11	83.5	194.8
				Peridotite and hybrid rocks					
WG5	PER	9/9	8.90	174.3	−58.6	6.4	59.08	71.9	188.0
WG6	PER	8/8	7.90	188.9	−62.9	3.6	204.94	76.2	146.2
WG7a	PER	7/7	6.90	176.1	−64.3	3.5	250.91	78.8	187.8
WG7b	PER	5/8	4.90	176.9	−69.2	6.6	108.78	85.4	197.8
WG8	PER	7/7	6.90	190.1	−63.7	2.2	624.88	76.7	141.2
WG9	HYB	9/9	8.90	173.7	−67.0	3.9	173.70	81.8	203.4
WG10	HYB	9/9	8.96	198.2	−65.8	3.5	21.98	75.8	115.2

Site – palaeomagnetic sampling location; n/N – ratio of samples used (n) to samples collected (N) at each site; R – resultant vector length, Dec/Inc – *in situ* declination and inclination; α_{95} – 95% confidence interval about the estimated mean direction, assuming a circular distribution; k – best estimate of (Fisher) precision parameter; corrected VGP Lat/Long – latitude and longitude of the virtual geomagnetic pole for the site; * – rejected: lightning struck; " – rejected: high dispersion (α_{95} >15 degrees, k < 15); # – excluded from group mean (greater than 2 sigma from mean). WGS – satellite Western Granite intrusion.

vectors involved 5 to 18 data points, but as few as 3 to as many as 25 were used. Magnetization vectors with maximum angular deviation values greater than 5° were not included in site mean calculations. For less than 10 % of the demagnetization results, it was necessary to anchor the magnetization vector to the origin. Individual sample directions were considered outliers and rejected from the site mean calculation if the angular distance between the sample direction and the estimated site mean was greater than 18°.

4.c. Principles of the AMS technique

An anisotropy of magnetic susceptibility measurement of one rock specimen yields an ellipsoid of magnetic susceptibility (K) defined by the length and orientation of its three principal axes, $K_1 \geq K_2 \geq K_3$, which are the three eigenvectors of the susceptibility tensor (Tarling & Hrouda, 1993). The long axis of the magnetic susceptibility ellipsoid, K_1, defines the magnetic lineation, while the short axis, K_3, defines the normal to the plane of the magnetic foliation. The

mean magnetic susceptibility (K_m) is the arithmetic mean of the principal axes K_1, K_2 and K_3. In addition, the AMS technique defines the degree of magnitude of the linear ($L = K_1/K_2$) and planar ($F = K_2/K_3$) fabric components. The technique also quantifies the corrected degree of anisotropy, $Pj = \exp(2[(\eta1 - \eta)^2 + (\eta2 - \eta)^2 + (\eta3 - \eta)2]^{1/2})$, where $\eta1 = \ln K1$, $\eta2 = \ln K2$, $\eta3 = \ln K3$, and $\eta = \ln(K1 + K2 + K3)^{1/3}$. A value of $P_j = 1$ describes a perfectly isotropic fabric, a P_j value of 1.15 describes a sample with 15 % anisotropy and so on. Given the above, P_j values of 0–5 % indicate a weak anisotropy, 5–10 % moderate anisotropy, 10–20 % a strong anisotropy, and > 20 % a very strong anisotropy. The shape of the susceptibility ellipsoid (T_j) (with $T_j = (2\ln k_2 - \ln k_1 - \ln k_3)/(\ln k_1 - \ln k_3)$: Jelinek, 1981) ranges from +1 where purely oblate to −1 where purely prolate, and is triaxial between both end-members.

We measured the AMS of 470 specimens prepared from samples collected at 27 sites distributed across the Western Granite, of which 401 yield interpretable results (Table 2). In addition, we measured the AMS of 99

Table 2. Anisotropy of magnetic susceptibility data from the Western Granite, NW Scotland

Site	Rock type	No.	N	Km	K1 (*in situ*)	K3 (*in situ*)	K1 (Cor)	K3 (Cor)	L	F	P	Pj	T	Sp	British Grid Ordnance Survey Latitude	Longitude	Elev (m)
WG1	WGS	10	13	68.63	297\3	180\83	7\9	291\79	1.021	1.015	1.037	1.037	−0.153	P	57.0089	6.3423	190
WG2*	WGS	10	10	62.87	45\16	160\56	41\15	175\69	1.007	1.024	1.030	1.032	0.561	O	57.0077	6.3407	190
WG3	WG	9	14	74.96	159\6	251\23	160\18	256\16	1.009	1.028	1.038	1.039	0.492	O	57.0032	6.3578	250
WG4	WG	9	11	36.08	340\10	245\25	160\2	251\20	1.009	1.019	1.028	1.029	0.378	O	57.0051	6.3601	255
WG5#	PER	0	12														350
WG6	PER	16	19	18.87	140\23	306\66	140\36	310\51	1.023	1.007	1.031	1.032	−0.506	P	56.9961	6.3650	350
WG7_a	PER	17	22	15.54	149\29	308\59	151\42	311\44	1.010	1.052	1.062	1.067	0.661	O	56.9961	6.3650	350
WG7_b#	PER	19	19	15.19	123\58	293\31	115\70	296\17	1.005	1.005	1.010	1.010	0.032	O	56.9961	6.3650	340
WG8	PER	12	13	55.59	89\20	332\51	85\28	329\36	1.006	1.014	1.020	1.020	0.367	O	56.9964	6.3655	330
WG9	HYB	9	14	90.33	35\12	291\48	33\9	296\34	1.008	1.012	1.021	1.021	0.182	O	56.9963	6.3666	350
WG10	HYB	18	21	51.55	225\1	316\20	225\1	316\5	1.008	1.023	1.031	1.032	0.466	O	56.9966	6.3668	360
WG11	WG	12	12	29.96	70\39	319\24	59\43	319\9	1.013	1.003	1.017	1.018	−0.583	P	56.9964	6.3685	380
WG12*	WG	21	22	15.74	159\63	50\10	176\74	47\10	1.004	1.010	1.014	1.014	0.484	O	57.0140	6.3805	365
WG13	WG	10	12	15.83	121\16	219\26	216\19	227\27	1.010	1.005	1.015	1.015	−0.287	P	57.0099	6.4050	270
WG14	WG	14	15	15.22	255\56	4\12	269\49	3\2	1.002	1.012	1.014	1.015	0.756	O	57.0102	6.4107	280
WG15	WG	17	18	9.872	206\22	308\28	212\26	309\13	1.009	1.002	1.011	1.012	−0.597	P	57.0112	6.4128	230
WG16	WG	17	18	15.07	304\45	177\31	306\32	185\42	1.006	1.012	1.018	1.018	0.380	O	57.0081	6.4136	320
WG17	WG	15	18	4.36	257\8	160\41	258\1	168\54	1.004	1.004	1.008	1.008	−0.053	P	57.0053	6.4216	310
WG18	WG	15	17	14.78	285\46	139\39	290\35	140\54	1.003	1.005	1.008	1.009	0.288	O	57.0027	6.4280	290
WG19*	WG	11	16	6.95	236\7	123\74	237\5	55\86	1.003	1.008	1.011	1.011	0.428	O	56.9993	6.4342	250
WG20	WG	16	18	13.96	306\61	100\26	309\48	94\38	1.006	1.007	1.013	1.013	0.026	O	57.0000	6.4341	250
WG21	WG	11	15	19.31	107\65	232\15	83\75	236\13	1.002	1.007	1.009	1.009	0.467	O	57.0012	6.4411	200
WG22	WG	15	18	21.41	244\33	146\13	251\28	147\28	1.006	1.010	1.016	1.017	0.283	O	57.0130	6.3780	300
WG23	WG	15	18	17.38	322\33	193\44	322\20	208\51	1.008	1.029	1.038	1.039	0.560	O	57.0094	6.3754	310
WG24	WG	18	20	20.73	358\30	227\49	354\20	244\47	1.003	1.010	1.013	1.014	0.561	O	57.0062	6.3673	310
WG25*	WG	15	16	35.08	145\26	272\52	146\39	282\40	1.003	1.027	1.030	1.033	0.788	O	56.9767	6.3893	50
WG26	WG	22	23	17.79	274\6	21\70	94\4	355\60	1.005	1.014	1.019	1.020	0.496	O	56.9797	6.3941	150
WG27	WG	13	15	49.82	308\74	121\15	312\61	119\29	1.011	1.018	1.030	1.030	0.218	O	56.9822	6.4004	170
WG28#	WG	0	16														150
WG29	WG	18	18	7.722	294\41	199\6	297\29	201\13	1.002	1.005	1.007	1.007	0.533	O	56.9962	6.4121	210
WG30	WG	22	24	40.46	187\11	303\67	290\19	308\52	1.006	1.013	1.019	1.019	0.361	O	56.9974	6.3712	400
WG31*	WG	11	15	21.58	325\9	222\56	145\4	244\54	1.003	1.012	1.015	1.016	0.637	O	56.9996	6.3731	400
WG32*	WG	20	20	10.53	13\59	177\30	359\50	184\41	1.002	1.009	1.010	1.011	0.698	O	57.0067	6.3782	450
WG33	PcGn	12	14	27.54	162\42	345\48	169\54	339\34	1.056	1.083	1.144	1.145	0.190	O	57.0021	6.3708	500
WG34	WG	17	17	10.16	350\40	248\14	345\29	251\8	1.003	1.009	1.012	1.013	0.527	O	57.0018	6.3716	530

Site – AMS sampling site; No. – number of samples collected at each site; N – number of accepted specimens at each site, typically, one to three specimens per sample; Km – magnitude of susceptibility (in 10E-3 SI); K1 (*in situ*) – *in situ* azimuth and plunge (in degrees) of magnetic lineation; K3 (*in situ*) – *in situ* azimuth and plunge (in degrees) of normal to magnetic foliation plane; K1 (Cor) and K3 (Cor) – tilt corrected K1 and K3 based on paleomagnetic data; L – magnetic lineation ((K1–K2)/Km); F – magnetic foliation ((K2–K3)/Km); P – anisotropy degree (K1/K3); Pj – magnitude of anisotropy, corrected anisotropy (Jelinek, 1981); T – shape parameter (Jelinek, 1981). Sp – shape: P – prolate shape; O – oblate shape; # – rejected site (high dispersion); * – K1–K2 confidence ellipse overlap (girdle), inferred magma flow direction of low confidence; WGS – satellite Western Granite intrusion; WG – Western Granite; PER – Peridotite; PcGn – Precambrian gneiss; HYB – hybrid.

Table 3. *Early Tertiary palaeomagnetic poles for northwest Scotland*

Rock type, location	Pole Latitude (N)	Longitude (E)	dp	dm	A95	K	Age (Ma)	Dec	Expected direction Inc	Reference
Northern England, Skye lavas	71.5	165.2	2.8	3.8			57.5	356.6	58.0	1
Northern England, Cleveland-Armathwaite dyke	75.0	240.0	5.5	5.5			58.5	21.1	66.4	2
Rhum and Canna igneous rocks	81.4	181.9	3.2	3.9			59.0	1.9	66.1	
Scotland, dy ke swarm, Skye	82.5	158.0	2.1	2.5			59.0	356.9	67.0	3
UK Ardnamurchan igneous complex	77.0	175.0	3.3	4.2			59.5	0.4	62.6	4
Scotland, Mull lavas	72.2	168.3	3.0	4.1			62.0	357.9	58.5	5
Synthetic poles	81.4	168.3			4.2	57.0	55	358.8	66.1	6
	80.5	188.9			4.3	48.8	60	3.7	65.6	6
	79.8	209.5			3.6	68.0	65	9.0	66.0	6

References: 1 – Willson, Hall & Dagley, 1972; 2 – Giddings, Tarling & Thomas, 1974; 3 – Dagley & Mussett, 1981; 4 – Dagley, Mussett & Skelhorn, 1984; 5 – Hall, Wilson & Dagley, 1977; 6 – Besse & Courtillot, 2002.
Semi-major (dm) and semi-minor (dp) axes of the confidence limits about the magnetic pole. Dec – declination; Inc – inclination; A95 – 95% confidence limit about the pole; K – best estimate of (Fisher) precision parameter.

specimens from samples at seven sites in the peridotite and hybrid rocks of which 73 yield interpretable results. All sample sites were collected away from faults and fractures and were precisely positioned using GPS (Table 2). AMS measurements were performed on a Kappabridge KLY-4S, operating at low alternating field 3.7×10^{-5} T (300 A/m) at 875 Hz at the University of New Mexico Paleomagnetism laboratory.

5. Results

5.a. Palaeomagnetic results

5.a.1. General demagnetization behaviour

Of the 27 sample sites in the Western Granite, 26 sites yield interpretable results (Table 1). The one rejected site (WG31) did not yield stable end-point behaviour and appears to have been lightning-struck. All seven sites in the peridotite and hybrid rocks yielded interpretable results. Overall, progressive alternating field response of all rocks is characterized by high-quality results (Fig. 5), with a linear trajectory defined over a broad range of peak fields. Duplicate specimens treated with thermal demagnetization yielded directional data similar to those resolved in AF demagnetization (Fig. 6). In general, most samples contain a single characteristic remanent magnetization (ChRM) that is well grouped at the site level, but some samples also contain additional magnetizations, depending on rock type, that are readily randomized by 10 mT or by 250 °C (Figs 5, 6). We interpret these magnetization components as low-coercivity viscous overprints (VRM). After removing the VRM, the ChRM, which we interpret as the primary thermal remanent magnetization (TRM), decays along a roughly univectoral path to the origin with less than 10 % of the NRM intensity remaining after treatment in 120 mT fields or by 600 °C (Figs 5, 6).

5.a.2. Palaeomagnetism

Of the 26 interpretable sites, 22 yield *in situ* reverse polarity mean directions (after inverting WG21 through

the origin) of south to southwest declination and moderate to steep inclinations that are well grouped (17 sites with $\alpha_{95} < 10°$) at the site level and provide an overall group mean D = 213.2°, I = −69.5°, R = 21.36, α_{95} = 5.5°, k = 33.2 (ASD = 14.05°) that is discordant, at 95 % confidence, to an early Paleocene expected field D = 183.7°, I = −65.6°, A95 = 4.3° based on a 60 Ma synthetic palaeomagnetic pole (Besse & Courtillot, 2002) (Fig. 7; Table 3). The discordant group mean is restored to the Paleocene expected field direction by removing an inferred 15° of northwest-side-down tilting about a best-fit horizontal tilt axis trending 040°.

All palaeomagnetic data from the peridotite and hybrid rocks yield *in situ* reverse polarity results of south declination and moderate negative inclinations that are very well grouped (five sites with $\alpha_{95} < 4°$) at the site level and provide an overall group mean D = 182.6°, I = −64.8°, R = 6.9741, α_{95} = 4.0°, k = 269.9, which is statistically indistinguishable from an early Paleocene expected field D = 183.7°, I = −65.6° (Besse & Courtillot, 2002) (Fig. 7).

5.a.3. Field test

To evaluate the antiquity of the magnetization, a palaeomagnetic contact test was conducted at a partially exposed margin of the intrusion where feldspathic peridotite is emplaced into the Western Granite just northeast of Ard Mheall (Fig. 2). Due to exposure limitations, an ideal contact test could not be performed; however, a modified test was attempted. We established sampling sites in the feldspathic peridotite at a distance of about 50 m from the inferred contact with the granite, and progressively closer to the intrusion. In total, five sites were established in feldspathic peridotite, two sites in hybrid rocks, and one site in the granite. The granite–peridotite contact is not a simple baked intrusive contact; rather it is a complex intrusion breccia, consisting of a narrow (< 10 m) zone of hybrid rocks that are a mixture of felsic and mafic material enveloping blocks of felsic and mafic rocks
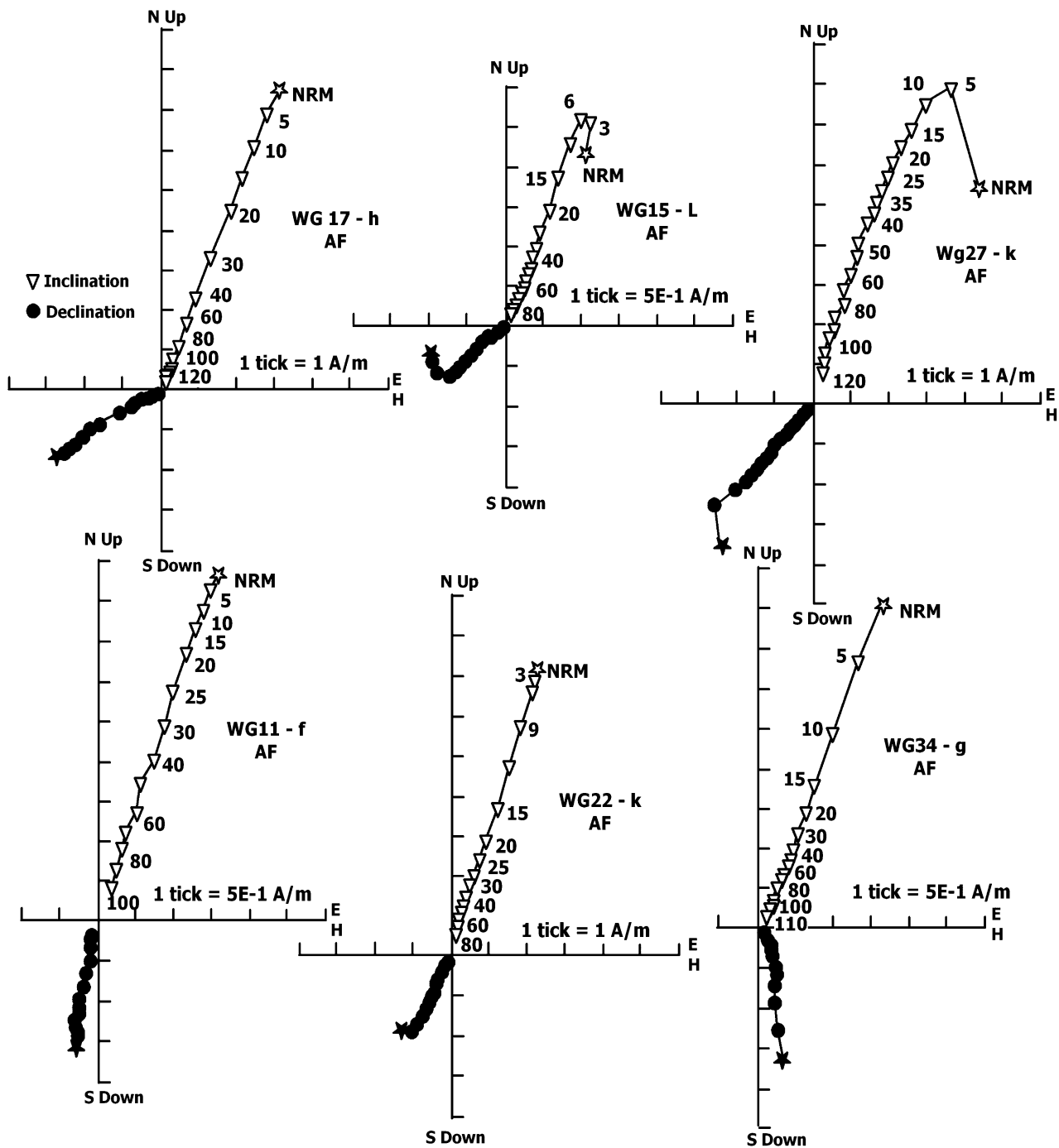
Figure 5. Representative *in situ* modified AF demagnetization diagrams (Zijderveld, 1967; Roy & Park, 1974). Solid (open) symbols represent the projection onto the horizontal (true vertical) plane. AF demagnetization steps are given in milliTesla and thermal demagnetization steps in degrees Celsius. Typically, AF and thermal demagnetization (TH) results from two specimens of the same sample are shown for comparison for some samples. See Figure 6 for TH demagnetization diagrams. Diagrams are designated by a Site number (e.g. WG13), method of treatment (AF or TH), and rock type. Intensity (A/m), is shown along one axis for each sample; each tick equals indicated intensity.

from < 1 cm to > 1 m in diameter. This zone reflects partial melting of the granite due to emplacement of the mafic peridotite (Greenwood, Donaldson & Emeleus, 1990; Emeleus & Troll, in press). From west to east, progressively closer to the peridotite contact zone, the granite yields mean directions for WG11 (187.8°, −70.0°), within the hybrid rocks, WG9 (173.7°, −67.0°) and WG10 (198.2°, −65.8°), and in the peridotite WG8 (190.1°, −63.7°), WG7b (176.9°, −69.2°), WG7a (176.1°, −64.3°), WG6 (188.9°, −62.9°), WG5 (174.3°, −58.6°). Overall, the remanence directions in the granite progressively shallow and become more south-directed, and more similar to those characteristic of the peridotite as the contact is approached. Although the data do not define a strict positive contact test, we interpret the progressive change in direction from cross-cutting feldspathic peridotite to host granite to indicate that the granite
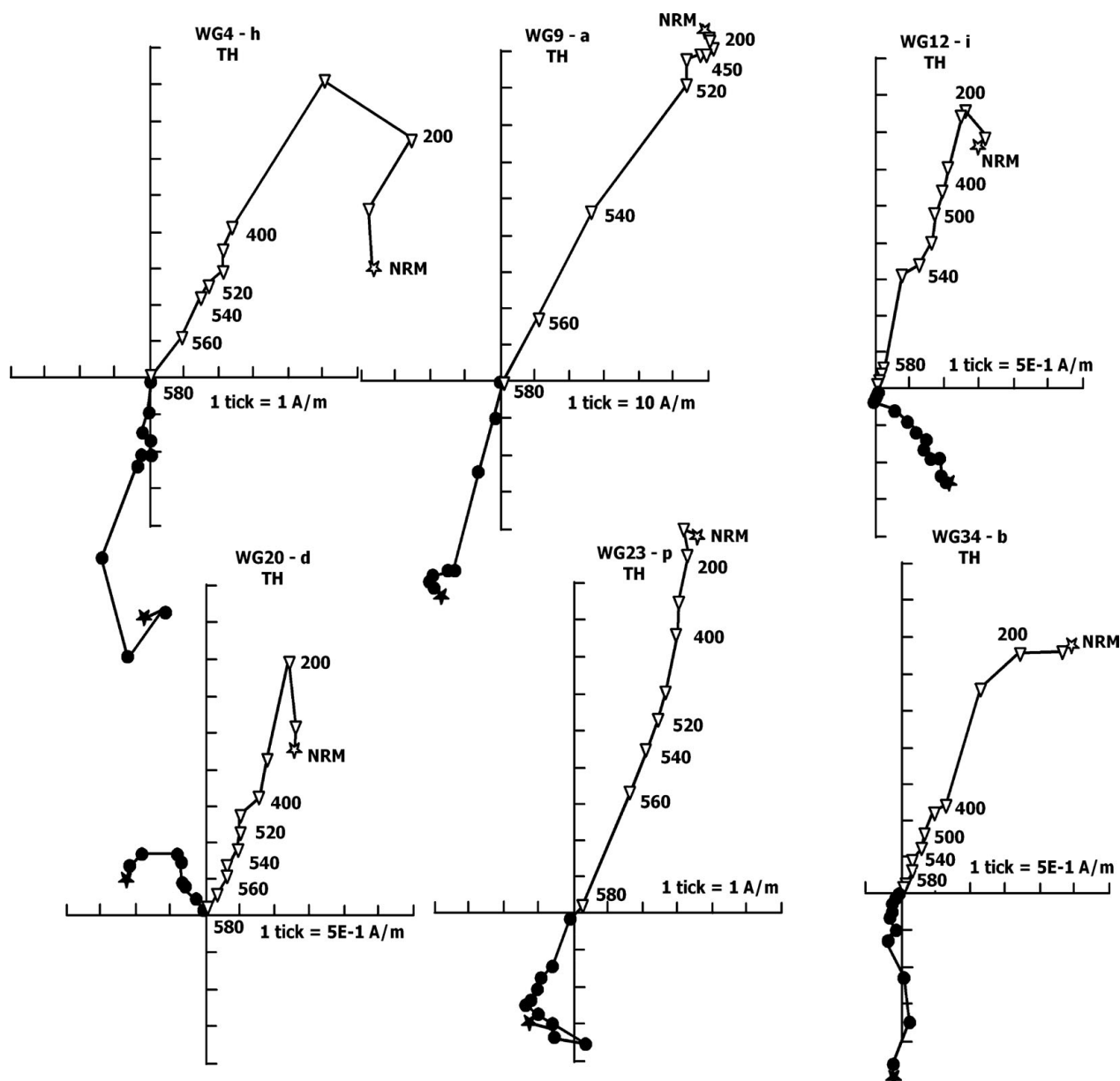
Figure 6. Representative *in situ* modified thermal (TH) demagnetization diagrams. For legend see Figure 5.

and peridotite have distinct remanence directions and thus that their ChRMs are primary.

5.b. Magnetic susceptibility results

5.b.1. General susceptibility behaviour

Several magnetic investigations of silicic plutonic rocks have shown that ferrimagnetic phases, such as magnetite and maghemite, dominate the magnetic susceptibility of such rocks (Rochette, Jackson & Aubourg, 1992; Tarling & Hrouda, 1993; Bouchez, 1997). In the Western Granite, petrographic observations, magnetic susceptibility measurements and rock magnetic experiments indicate that magnetite and titanomagnetite are the most common ferromagnetic phases (Fig. 4).

Rock magnetic data (IRM acquisition, hysteresis data, high and low temperature susceptibility, and three-component IRM acquisition) indicate that the remanence and the AMS fabrics in the Western Granite are likely carried and defined by a ferromagnetic phase, likely low-Ti magnetite, having a limited domain state and grain size (M. S. Petronis, unpub. data). Low-temperature susceptibility experiments show little to no temperature-dependent behaviour, indicating that a ferromagnetic phase(s) dominated the AMS fabric with minor contribution from the paramagnetic phases (Richter & van der Pluijm, 1994). The high bulk susceptibility (Table 2) further indicates that a ferromagnetic phase (e.g. magnetite) is the principal magnetic mineral which dominates the susceptibility of these rocks. The remaining Fe-bearing phases, predominantly Fe–Mg silicates such as hornblende and pyroxene, are paramagnetic and thus contribute significantly less to the magnetic susceptibility. This is because large values of K_{mean} of these rocks (e.g. 26.26×10^{-3} SI average magnitude) are consistent
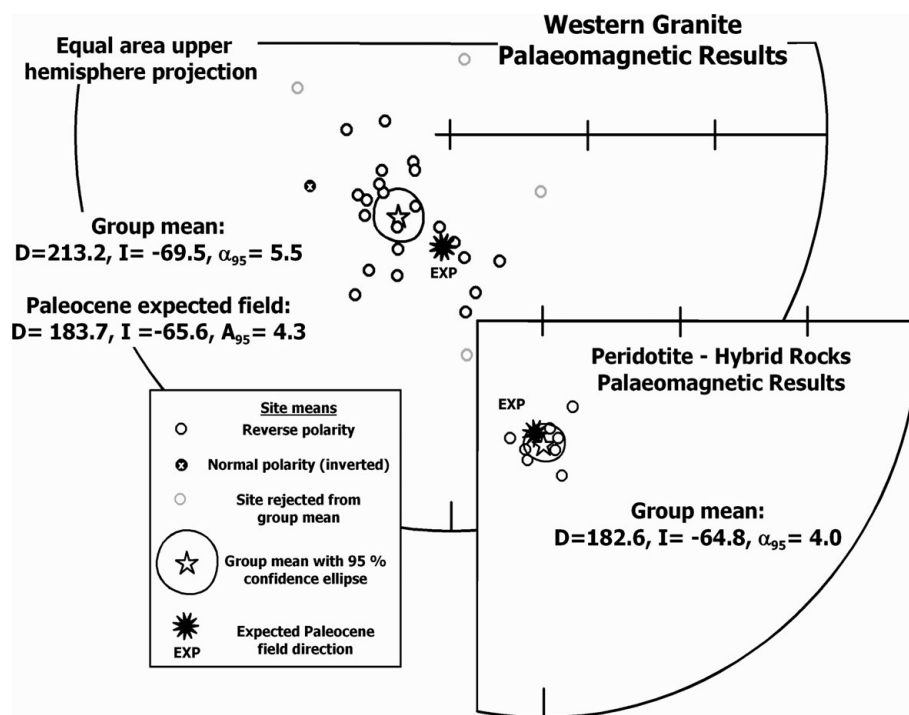
Figure 7. Equal area projection of *in situ* site mean paleomagnetic results from the Western Granite, peridotite, and hybrid rocks. Sites means and expected directions are projected onto the upper hemisphere.

with a dominance by ferromagnetic phases (Rochette, 1987), and more generally, ferromagnetic minerals have susceptibilities orders of magnitude higher than paramagnetic minerals (Uyeda *et al.* 1963; Hrouda, 1982; Dekkers, 1990; Heider, Zitzelberger & Fabian, 1996).

Magnetic susceptibility data for all sites in the Western Granite rocks are given in Table 2, together with the other principal magnetic features measured. Bulk magnetic susceptibilities of individual sites throughout the Western Granite range between 4.4×10^{-3} SI and 74.9×10^{-3} SI. In general, the highest values of K_{mean} are typically observed in sites in the east and south parts of the intrusion, though it is impossible to refine this observation any further without a higher-resolution dataset. K_{mean} is broadly proportional to the mode of magnetite in the rock (Balsley & Buddington, 1958), and the magnetic susceptibility values of the Western Granite samples suggest that the susceptibility (and hence the anisotropy) is dominated by a ferromagnetic phase, likely magnetite, in quantities of up to 3 modal %.

5.b.2. Degree of anisotropy and AMS ellipsoid shape

The corrected degree of anisotropy (P_j) measured for the Western Granite rocks varies between 1.01 and 1.04, and averages about 1.02. The magnetic fabric, although exhibiting markedly consistent values of P_j, is weak in strength, between 1.01 and 1.04 for 19 of 27 (76 %) sites measured. All sites with $P_j > 1.03$ are from the east and south parts of the intrusion, emphasizing the sample grouping referred to on the basis of K_{mean}

above. The shape parameter (T_j) describes, in general, a narrow range of AMS susceptibility ellipsoid shapes (Table 2). Although a range in the data between − 0.6 and 0.8 is observed, only 4 of 27 sites (14 %) are prolate ($T_j < 0$) with 19 sites yielding $T_j > 0$ (T_j mean = 0.33, n = 27). The susceptibility ellipsoids are therefore dominantly triaxial-to-oblate, suggesting that the planar element of the magnetic fabric dominates. Weak positive correlations are observed between T_j and K_{mean} and between T_j and P_j, again serving to highlight that, in general, the samples with the highest values of K_{mean} and P_j (in the south and east of the Western Granite) are those with the highest values of T_j, suggesting the most oblate susceptibility ellipsoids. Conversely, those samples in the western part of the intrusion exhibit more triaxial magnetic fabric shapes, lower anisotropy degree and lower values of K_{mean}.

5.b.3. Magnetic foliations and lineations

The AMS fabric elements in Table 2 are tilt corrected, based on the palaeomagnetic data, using an inferred tilt axis (040, 15NW) to their original, pre-tilt orientation. Magnetic foliation (K_1–K_2) planes often strike sub-parallel to the outer margin of the granite and dip moderately to steeply outward (Fig. 8). Exceptions to this are at two sites in the north of the intrusion (WG14 and WG15) and also site WG29 to the west (Fig. 8; Table 2). Magnetic lineations define two main fabric groups (Fig. 8). One lineation trend, mainly defined by sites in the eastern part of the intrusion, is oriented north–south and plunges gently to moderately. The other magnetic lineation trend is defined by data
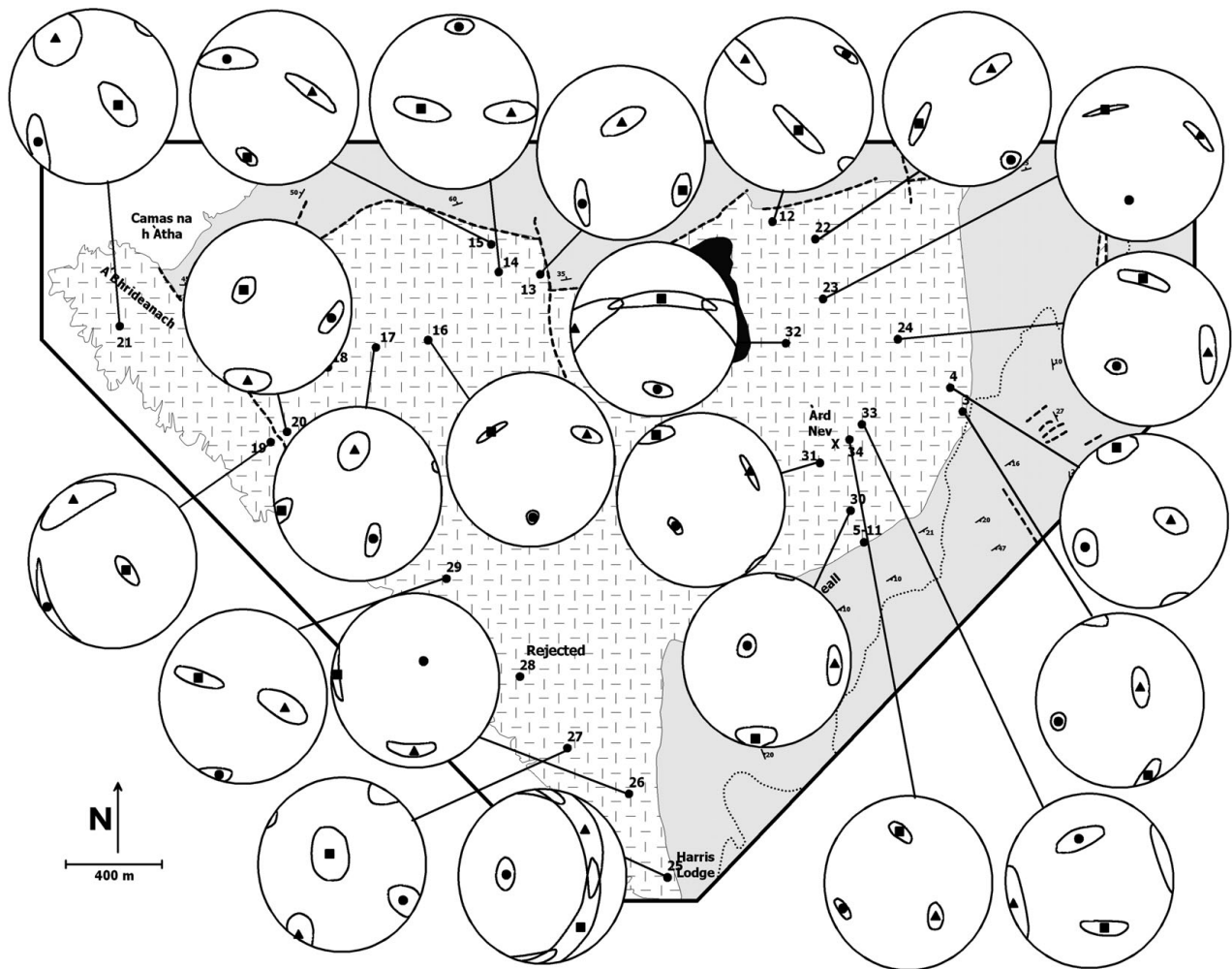
Figure 8. AMS results. Lower hemisphere equal area projections of *in situ* AMS principal susceptibility axes (max K$_1$, squares, intermediate K$_2$, triangles, and minimum K$_3$, circles) for all sites in the Western Granite. Sites WG5 to WG11 are not shown. For legend see Figure 2.

from sites in the south and west of the pluton, and is east–west and plunges in most cases to the west (though orientations are more inconsistent), at shallow to moderate angles (Fig. 8). Notably, the two groups of magnetic fabrics are broadly consistent with the two principal groups distinguished above by magnitudes of AMS parameters (T$_j$ and P$_j$) and bulk susceptibility (K$_{mean}$) (Table 2).

6. Discussion

6.a. Palaeomagnetism

Twenty-two of 26 sites in the Western Granite provide a group mean magnetization of south–southwest declination, moderate to steep negative inclination (D = 213.2°, I = −69.5°, α_{95} = 5.5°) (Fig. 7). The four sites (Table 1) excluded from the group mean have well-defined site mean directions but they are separated by over two angular standard deviations from the overall group mean of the other 22 sites. The group mean magnetization direction differs from any early Paleocene-age expected direction for this area based on synthetic poles and palaeomagnetic pole estimates for

northern Scotland (Table 3). We interpret the modified contact test as a positive result that shows that the remanence in the Western Granite is distinct from the remanence of parts of the younger Layered Suite. Based on these data, and isotopic age data (Chambers, Pringle & Parrish, 2005), the age of remanence acquisition is likely to be early Paleocene for both rock types. The Western Granite yields 21 of 22 sites of reverse polarity and one site of normal polarity, indicating, at face value, that cooling of the granite spanned at least one polarity reversal; however, even crude estimates of the duration of sampling of the geomagnetic field during cooling of the intrusion are not straightforward. Field observations and petrology indicate that the granite was likely emplaced at a shallow depth and thus cooled relatively quickly, yet, as argued below, over sufficient time to provide a time-averaged Paleocene field direction. The statistically distinct palaeomagnetic directions from the peridotite and hybrid rocks indicate that remanence acquisition in the granite occurred prior to emplacement of these rocks and that tilting of the Western Granite and associated host country rock occurred prior to or likely during emplacement of the Layered Suite (Fig. 9).
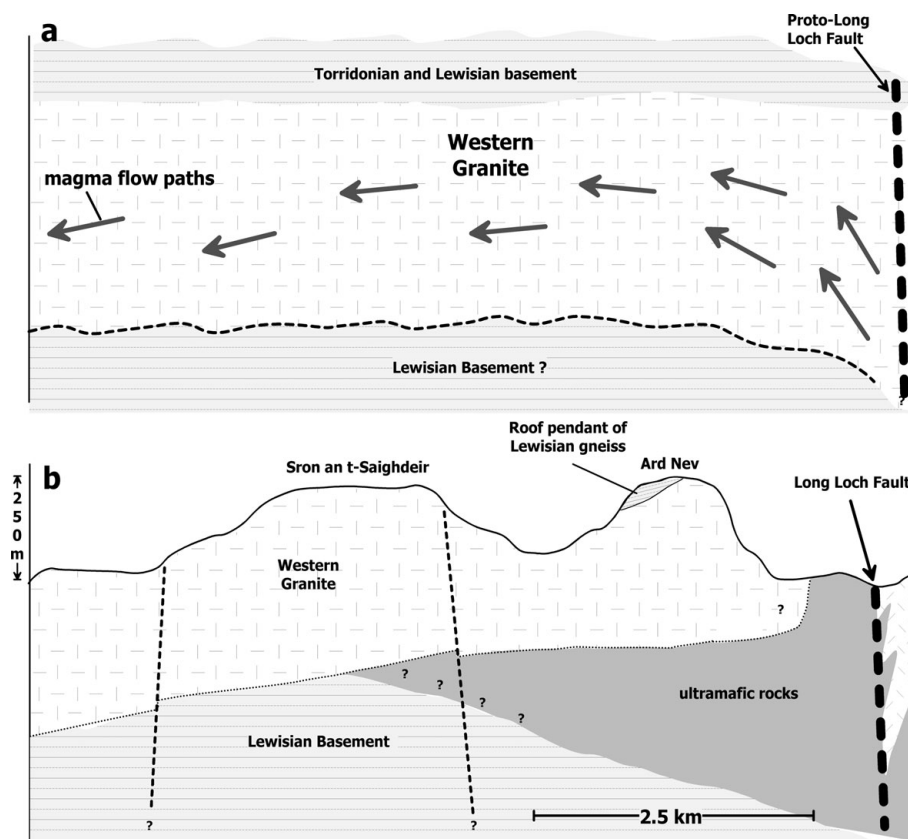
Figure 9. Interpretive diagram depicting inferred magma flow model that led to the formation of the Western Granite. (a) Emplacement of the Western Granite at shallow depth. The magma likely flowed up along the proto-Long Loch fault (or splay) and possibly exploited the Lewisian–Torridonian unconformity. (b) The inferred tilt recorded in the Western Granite, which did affect the adjacent ultrabasic rocks. The emplacement of the ultrabasic rocks at a shallow level caused significant distortion and local remobilization of the country rocks, and northwest-side-down tilting of the granite. Line of cross-section shown in Figure 10a.

Using palaeosecular variation (PSV) models (e.g. Merrill & McElhinny, 1983) for the average palaeolatitude of the study area ($\sim 47.0\,\text{N}°$), the virtual geomagnetic pole (VGP) angular standard deviation is predicted to be some $17°$ to $19°$, although secular variation in the Early Tertiary is not well constrained. The VGP angular standard deviation of our dataset in the granite (22 accepted sites) is $21.8°$, which is above the predicted range. One potential contribution to the observed dispersion of the site mean directions, which is difficult to assess, is that of intrapluton, subsolidus deformation after ChRM acquisition. We doubt that this is an important contribution because of the lack of identified structures along which appreciable offset may have taken place. The data from the seven sites in the peridotite and hybrid rocks yield distinct palaeomagnetic directions from the Western Granite, and the group mean ($D = 182.6°$, $I = -64.8°$) is statistically indistinguishable from the late Paleocene expected field direction. We interpret the palaeomagnetic data from the peridotite and hybrid rocks to indicate no post-emplacement tilting of these rocks since remanence acquisition. We argue that the magnetization sampled a geomagnetic field distinct from the Western Granite and the group mean provides a reasonable average of the early Palaeogene field.

6.b. Implications for the Rum igneous centre

Accepting that the magnetization characteristic of the Western Granite adequately averages a Paleocene geomagnetic field, the group mean result differs, in both declination and inclination, from expected directions based on palaeomagnetic pole estimates for the northern United Kingdom for the time period between the early and late Paleocene (Table 3). For example, using the 60 Ma synthetic pole of Besse & Courtillot (2002), which provides an expected direction of $183.7°$, $-65.6°$ (A95 = $4.3°$), we estimate a declination difference (inferred rotation, R) of $+29.2°$ $\pm 13.8°$, and a minimum inclination difference (inferred flattening, F) of $-3.5 \pm 5.1°$ (Beck, 1980; Demarest, 1983). Expected directions based on other Paleocene palaeomagnetic poles are of similar declination and inclination (Table 3), and thus would result in rotation and flattening estimates that are indistinguishable from the estimate using the synthetic palaeomagnetic pole of Besse & Coutillot (2002). One exception is the *c.* 58.5 Ma palaeomagnetic pole from northern England based on data from the Cleveland–Armathwaite dykes (Giddings, Tarling & Thomas, 1974; Table 3). The difference between observed directions in the Western Granite and a Paleocene expected direction is most logically explained by horizontal axis tilting or a

combination of moderate clockwise vertical axis rotation and tilting. We note that simple clockwise rotation does not account for the modest inclination discordance (Fig. 7). About 15° of northwest-side-down tilt about a northeast-trending (040°) horizontal tilt axis fully explains the discrepancy and is consistent with field relations and emplacement models of the Rum Central Complex (Emeleus *et al.* 1996) (Fig. 9). The inferred tilt we conclude to be recorded in the Western Granite is consistent with a cause and effect relationship, particularly when considering the field relations between the granite and the ultrabasic rocks. We argue that the emplacement of the ultrabasic rocks at a shallow level caused roof uplift and associated tilting of the Western Granite, providing space for mafic magma emplacement (Fig. 9).

6.c. Anisotropy of magnetic susceptibility

AMS studies have been successfully applied to the shallow-level intrusions of the British Palaeogene Igneous Province over the past several years (e.g. Geoffrey, Olivier & Rochette, 1997; O'Driscoll *et al.* 2006; Stevenson *et al.* 2007). The latter two of these studies questioned the validity of long-standing ring-dyke models in the Ardnamurchan (NW Scotland) and Eastern Mourne (Northern Ireland) igneous centres, respectively. In particular, Stevenson *et al.* (2007) interpreted gently outward-dipping magnetic fabrics in the Eastern Mourne granite pluton, even close to contacts, as reflecting a forceful laccolithic style of emplacement. This laccolith model is supported by field evidence for deflection and uplift of country rock bedding close to the intrusion margins. Conversely, O'Driscoll *et al.* (2006) interpreted consistently inward-plunging magnetic lineations, inward-dipping contacts and inward-dipping magmatic layering in the mafic Great Eucrite of Centre 3, Ardnamurchan as reflecting a lopolithic geometry. Geoffrey, Olivier & Rochette (1997) found that magnetic foliations in the Western Red Hills granite sheets on the Isle of Skye igneous centre dip gently yet steepen to outward dips approaching the outer wall of each intrusion. The authors interpreted this fabric as a post-injection magmatic fabric, indicative of upward-directed magma pressure. Geoffrey, Olivier & Rochette (1997), however, did not dispute the established ring-dyke emplacement mechanism, and accepted that the contacts of the Western Red Hills granite were near vertical (after Bell, 1979).

In the Western Granite AMS dataset, we recognize two subtle groupings, and these are distinguishable on the basis of both the magnetic fabric and magnitude of susceptibility parameters (Fig. 10a, b). One of these groups is defined by the data from rocks principally exposed in the eastern and southern parts of the Western Granite, and is characterized by comparatively higher bulk susceptibilities (K_{mean}), relatively strong anisotropies (P_j), and oblate susceptibility ellipsoids. The second group, characterized by rocks from western part exhibits lower values of K_{mean} and P_j, and sus-

ceptibility ellipsoids that are triaxial in shape (Table 2). Both magnetic fabric groups also show a distinction in magnetic lineation data, although only one pattern can be extracted from the magnetic foliation data: dipping moderately to steeply outward and striking sub-parallel to the outer margins of the intrusion (Fig. 10). The first group of magnetic lineation data (representing rocks in the eastern part of the intrusion) trends approximately north–south and plunges in either direction (Fig. 10a). The second group of magnetic lineations are more inconsistently oriented, though an overall east–west trend is observed. We suggest that the more oblate fabrics in the east part of the intrusion reflect somewhat higher magmatic strain, perhaps closer to the roof of the intrusion (note the close proximity of the Lewisian gneiss pendant). We infer that the magnetic lineations indicate a magma flow direction, and suggest emplacement of the intrusion from the south–southeast.

We propose a model in which most magnetic foliation observations are consistent with some up-doming of the granite body during/following emplacement (Fig. 10b). This hypothesis is supported by the outward-dipping Torridonian strata to the north of the Western Granite, which appear to be deflected into parallelism with the contacts of the granite (Fig. 10b). Bedding in the Torridonian throughout the rest of the island exhibits a gently westward (and regionally consistent) dip orientation, so that rotation by the granite seems like the most likely mechanism for the observed change in the strike of the country rock. It is worth noting that similar bedding orientations at the margins of granite laccoliths and other intrusions have been described where magma emplacement was interpreted to represent inflation of a granite sheet during a laccolithic style of emplacement (Corry, 1988).

It is not, however, immediately obvious how to interpret the magnetic lineations in the context of a dome-like intrusion, though we suggest that they represent magma flow for the reasons outlined above. It is possible that during doming of the granite, lineations were not significantly affected by this process, apart from some modification of the magnitude of plunge observed, giving rise to the slightly irregular plunges observed in the data. Though there are two likely major structural ascent locations for the Western Granite magma, the Main Ring Fault and the Long Loch Fault (see Figs 1, 2), the data do not immediately identify either one as a probable candidate (Fig. 10). This is because the data argue for a source area located to the south–southeast (Fig. 10). The Long Loch fault system is suggested to have sited emplacement of the younger Layered Suite (Emeleus *et al.* 1996; O'Driscoll *et al.* 2007), so it is possible that late movement on the Long Loch Fault modified the magnetic lineation directions in the east of the Western Granite (Group 1) to some extent. The linear elements of the magnetic fabric are generally better defined than those of the first group, giving rise to triaxial susceptibility ellipsoids, though the orientations are not as consistent. This leads to our interpretation that the second group of data reflects
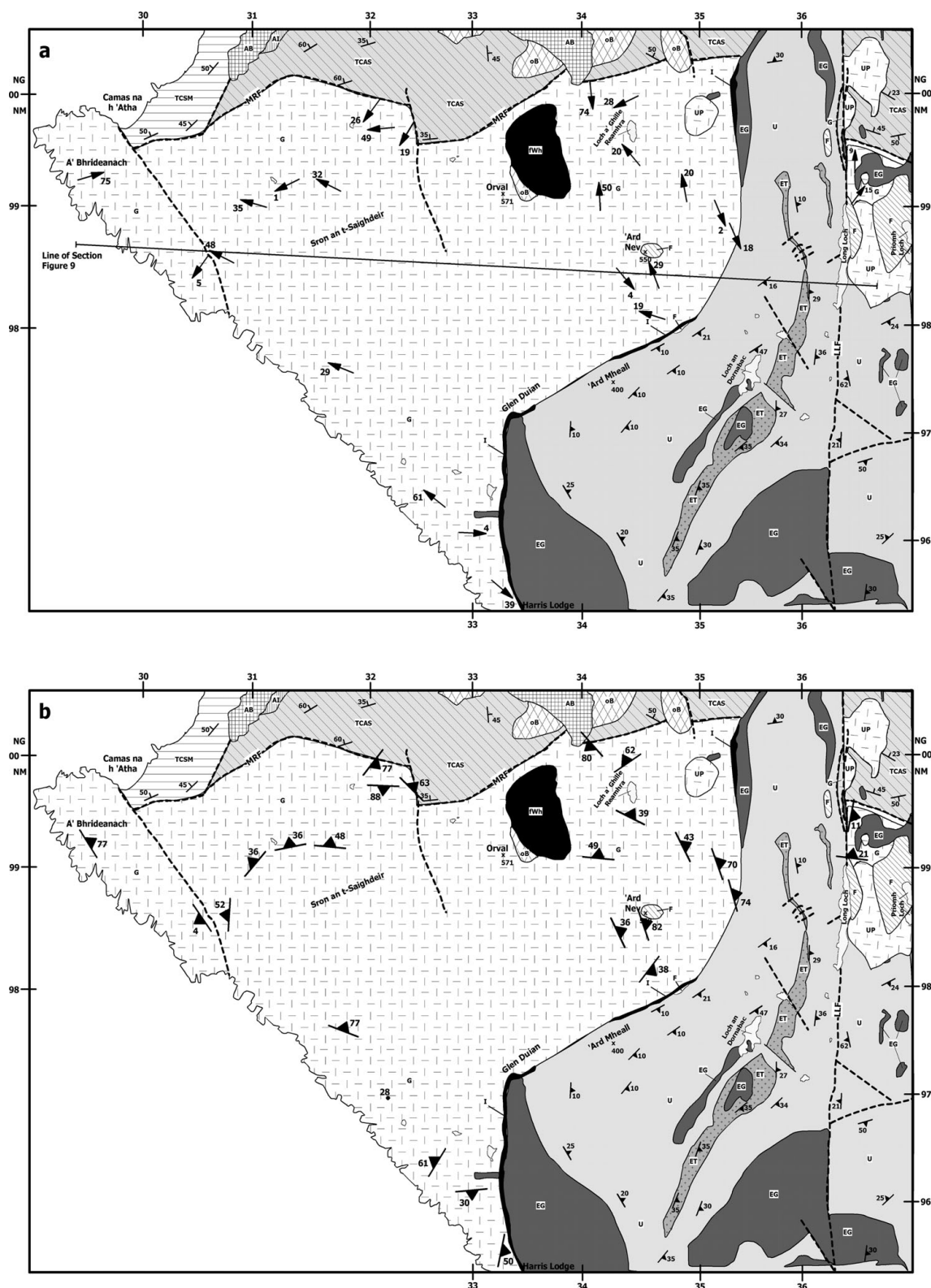
Figure 10. Simplified geological map depicting AMS magnetic lineation and foliation data from the Western Granite. Sites established in the eastern and southern parts of the Western Granite are characterized by high bulk susceptibilities, strong anisotropies and oblate susceptibility ellipsoids. Sites from the western part exhibits lower susceptibility and anisotropy values and triaxial susceptibility ellipsoids (Table 2). (a) Magnetic lineation data. Sites in the eastern part of the intrusion yield lineations that trend north–south and plunge gently to moderately. For sites in the south and west, lineations trend east–west and plunge shallowly to moderately, dominantly toward the west. The triaxial fabrics and gentler plunge of the magnetic lineations in the west are interpreted to reflect lateral flow transport. (b) Magnetic foliations, defined by the K1–K2 plane, typically strike sub-parallel to the outer margin of the granite and dip moderately to steeply outward towards the contact of the granite. The magnetic foliations reflect a record of up-doming of the granite body during emplacement. The outward-dipping Torridonian strata to the north appears to be deflected into parallelism with the contacts of the granite supporting this interpretation. The Long Loch fault system exhibits a similar north–south trend to the trend of the AMS lineations from the eastern part of the intrusion and it (or a similarly oriented splay) plausibly served as a conduit for magma emplacement or a concealed structure to the south–southeast. For legend see Figure 2.

semi-lateral sub-horizontal flow of magma filling a tabular granite sheet (Fig. 10) in a zone of slightly lower magmatic strain. If the gneiss pendant on Ard Nev represents roof material and an original intrusive contact, then it might be expected that slightly more oblate fabrics would be observed in the east. Given the inferred tilt from the palaeomagnetic data presented here, the sites in the west of the intrusion might be sampling a zone of the intrusion further from the roof.

7. Conclusions

Palaeomagnetic data are discordant to the early Palaeogene expected field, and we interpret these data to indicate that the Western Granite as a whole was tilted to the northwest by about $15°$. The slightly younger ultrabasic rocks of the Rum Layered Suite yield palaeomagnetic data that are indistinguishable from the expected field and thus indicate no post-emplacement deformation since early Palaeogene times. The inferred tilt recorded in the Western Granite, which did not affect the younger ultrabasic suite, suggests that emplacement of the Rum Layered Suite rocks caused significant distortion and local remobilization of the country rocks coupled with roof uplift and tilting of the Western Granite to accommodate the intrusion. The AMS data from the Western Granite reveal magnetic lineations that indicate flow from a source to the south–southeast, and this cannot readily be linked to either of the major structures in the area, the Long Loch Fault or the Main Ring Fault. The magnetic foliations together with the observed deformation (deflection) of the country rock in the north suggest a degree of doming of the granite roof during intrusion, possibly accompanied by failure and faulting on the periphery of the roof-zone.

References

BAILEY, E. B. 1945. Tertiary igneous tectonics of Rhum (Inner Hebrides). *Quarterly Journal of the Geological Society of London* **100**, 165–91.

BAILEY, E. B., CLOUGH, C. T., WRIGHT, W. B., RICHEY, J. E. & WILSON, G. V. 1924. *Tertiary and Post-Tertiary geology of Mull, Loch Aline and Oban*. Memoir of the Geological Survey of Great Britain, Sheet 44, Scotland, 445 pp.

BALSLEY, J. R. & BUDDINGTON, A. F. 1958. Iron titanium oxide minerals, rocks, and aeromagnetic anomalies of the Adirondack area, New York. *Economic Geology* **53**(7), 777–805.

BECK, M. E. 1980. Palaeomagnetic record of plate-margin tectonic processes along the western edge of North America. *Journal of Geophysical Research* **85**, 7115–31.

BELL, J. D. 1979. Granites and associated rocks of the eastern part of the Western Redhills Complex, Isle of Skye. *Transactions of the Royal Society of Edinburgh* **66**, 307–43.

BESSE, J. & COURTILLOT, V. 2002. Apparent and true polar wander and the geometry of the geomagnetic field over the last 200 Myr vol 107, art no 2300, 2002. *Journal of Geophysical Research – Solid Earth* **108**, 2469.

BLACK, G. P. 1952. The age relationship of the granophyre and basalt of Orval, Isle of Rhum. *Geological Magazine* **89**, 106–12.

BLACK, G. P. 1954. The acid rocks of western Rhum. *Geological Magazine* **91**, 257–72.

BLAKE, D. H., ELWELL, R. W. D., GIBSON, I. L., SKELHORN, R. R. & WALKER, G. P. L. 1965. Some relationships resulting from the intimate association of acid and basic magmas. *Quarterly Journal of the Geological Society of London* **121**, 31–49.

BOUCHEZ, J. L. 1997. Granite is never isotropic: an introduction to AMS studies of granitic rocks. In *Granite: From Segregation of Melt to Emplacement Fabrics* (eds J. L. Bouchez, D. H. W. Hutton & W. E. Stephens), pp. 96–112. Dordrecht: Kluwer.

CHAMBERS, L. M., PRINGLE, M. S. & PARRISH, R. R. 2005. Rapid formation of the Small Isles Tertiary centre constrained by precise $^{40}Ar/^{39}Ar$ and U–Pb ages. *Lithos* **79**, 367–84.

CORRY, C. E. 1988. *Laccoliths – mechanics of emplacement and growth*. Geological Society of America, Special Paper no. 220, 120 pp.

DAGLEY, P. & MUSSETT, A. E. 1981. Palaeomagnetism of the British Tertiary igneous province: Rhum and Canna. *Geophysical Journal of the Royal Astronomical Society* **65**, 475–91.

DAGLEY, P., MUSSETT, A. E. & SKELHORN, R. R. 1984. The palaeomagnetism of the Tertiary igneous complex of Ardnamurchan. *Geophysical Journal of the Royal Astronomical Society* **79**, 911–22.

DEKKERS, M. J. 1990. Magnetic properties of natural goethite-III Magnetic behaviour and properties of minerals origionating from goethite dehydration during thermal demagnetization. *Geophysical Journal International* **103**, 233–50.

DEMAREST, H. H. 1983. Error analysis for the determination of tectonic rotations from palaeomagnetic data. *Journal of Geophysical Research* **88**, 4321–8.

DONALDSON, C. H., TROLL, V. R. & EMELEUS, C. H. 2001. Felsites and breccias in the Northern Marginal Zone of the Rum Igneous Complex: changing views ca. 1900–2000. *Proceedings of the Yorkshire Geological Society* **53**, 167–75.

DUNHAM, A. C. 1968. The felsites, granophyre, explosion breccias and tuffisites of the north eastern margin of the Tertiary igneous complex of Rhum, Inverness-shire. *Quarterly Journal of the Geological Society of London* **123**, 327–52.

EMELEUS, C. H. 1994. *1:20 000 solid geology map of Rum, 2nd edition*. Edinburgh: Scottish Natural Heritage.

EMELEUS, C. H. 1997. *Geology of Rum and the adjacent islands*. Memoir of the British Geological Survey, Sheet 60 (Scotland), 170 pp.

EMELEUS, C. H., CHEADLE, M. J., HUNTER, R. H., UPTON, B. G. J. & WADSWORTH, W. J. 1996. The Rum Layered Suite. In *Layered igneous rocks* (ed. R. G. Cawthorn), pp. 403–40. Amsterdam: Elsevier.

EMELEUS, C. H., DUNHAM, A. C. & THOMPSON, R. N. 1971. Iron-rich pigeonites from acid rocks in the Tertiary Igneous Province of Scotland. *American Mineralogist* **56**, 940–51.

EMELEUS, C. H. & TROLL, V. In press. *Excursion Guide to the Paleocene Igneous Rocks of the Isle of Rum, Inner Hebrides*. Edinburgh: Edinburgh Geological Society.

ENGLAND, R. W. 1992. The genesis, ascent, and emplacement of the Northern Arran Granite, Scotland: Implications for granitic diapirism. *Geological Society of America Bulletin* **104**, 606–14.

GAMBLE, J. A. 1979. Some relationships between coexisting granitic and basaltic magmas and the genesis of hybrid rocks in the Tertiary central complex of Slieve Gullion, northeast Ireland. *Journal of Volcanology and Geothermal Research* **5**, 297–316.

GAMBLE, J. A., MEIGHAN, I. G. & MCCORMICK, A. G. 1992. The petrogenesis of tertiary microgranites and granophyres from Slieve Gullion Central Complex, NE Ireland. *Journal of the Geological Society, London* **149**, 93–106.

GEIKIE, A. 1897. *The ancient volcanoes of Great Britain*. London: Macmillan, 2 vols, xxiv + 477 pp., viii + 492 pp.

GEOFFREY, L., OLIVIER, P. & ROCHETTE, P. 1997. Structure of a hypovolcanic acid complex inferred from magnetic susceptibility anisotropy measurements: the Western Red Hills granites Skye, Scotland, Thulean Igneous Province. *Bulletin of Volcanology* **59**, 147–59.

GIDDINGS, J. W., TARLING, D. H. & THOMAS, D. H. 1974. The palaeomagnetism of the Cleveland-Armathwaite Dyke, northern England. *Transactions of the Nature Society, Northumberland* **4**, 220–6.

GREENWOOD, R. C., DONALDSON, C. H. & EMELEUS, C. H. 1990. The contact zone of the Rum ultrabasic intrusion: evidence of peridotite formation from magnesian magmas. *Journal of the Geological Society, London* **147**, 209–12.

HALL, J. M., WILSON, R. L. & DAGLEY, P. 1977. A palaeomagnetic study of the Mull Lava succession. *Geophysical Journal of the Royal Astronomical Society* **49**, 499–514.

HARKER, A. 1904. *The Tertiary igneous rocks of Skye*. Memoir of the Geological Survey of Great Britain. Sheets 70 and 71 (Scotland), 471 pp.

HARKER, A. 1908. *The geology of the Small Isles of Inverness shire*. Memoirs of the Geological Survey: Scotland. Sheet 60 (Scotland), 210 pp.

HEIDER, F., ZITZELBERGER, A. & FABIAN, K. 1996. Magnetic susceptibility and remanent coercive force in grown magnetite crystals from 0.1 μm to 6 mm. *Physics of the Earth and Planetary Interiors* **93**, 239–56.

HROUDA, F. 1982. Magnetic anisotropy of rocks and its applications in geology and geophysics. *Geophysical Survey* **5**, 38–82.

HUGHES, C. J., WADSWORTH, W. J. & EMELEUS, C. H. 1957. The contact between Tertiary granophyre and Torridonian arkose on Minishal, Isle of Rhum. *Geological Magazine* **94**, 337–9.

HUGHES, C. J. 1960. The Southern Mountains igneous complex, Isle of Rhum. *Journal of the Geological Society, London* **116**, 111–38.

JELINEK, V. 1981. Characterization of the magnetic fabric of rocks. *Tectonophysics* **79**, T63–7.

JUDD, J. W. 1889. The Tertiary volcanoes of the Western Isles of Scotland. *Quarterly Journal of the Geological Society of London* **45**, 187–219.

KIRSHVINCK, J. L. 1980. The least-squares line and plane and the analysis of palaeomagnetic data. *Geophysics Journal International* **62**, 699–718.

MCCORMICK, A. G., FALLICK, A. E., HARMON, R. S., MEIGHAN, I. G. & GIBSON, D. 1993. Oxygen and hydrogen isotope geochemistry of the Mourne Mountains Tertiary Granites, Northern Ireland. *Journal of Petrology* **34**, 1177–1202.

MEIGHAN, I. G. 1979. The acid igneous rocks of the British Tertiary Province. *Bulletin of the Geological Survey of Great Britain* **70**, 10–22.

MEIGHAN, I. G., FALLICK, A. E. & MCCORMICK, A. G. 1992. Anorogenic granite magma genesis: new isotope data for the southern sector of the British Tertiary Igneous Province. *Transactions of the Royal Society of Edinburgh* **83**, 227–33.

MERRILL, R. T. & MCELHINNY, M. W. 1983. *The Earth's Magnetic Field: Its History, Origin, and Planetary Perspective*. International Geophysical Series, vol. 32. Academic Press, 401 pp.

O'DRISCOLL, B., TROLL, V. R., REAVY, R. J. & TURNER, P. 2006. The Great Eucrite intrusion of Ardnamurchan, Scotland: re-evaluating the ring-dyke concept. *Geology* **34**, 189–92.

O'DRISCOLL, B., HARGRAVES, R. B., EMELEUS, C. H., TROLL, V. R., DONALDSON, C. H. & REAVY, R. J. 2007. Magmatic lineations inferred from anisotropy of magnetic susceptibility fabrics in Units 8, 9 and 10 of the Rum Eastern Layered Series, Scotland. *Lithos* **98**, 27–44.

PEACOCK, G. W., PETRONIS, M. S. & GEISSMAN, J. W. 2006. Anisotropy of Magnetic Susceptibility and Paleomagnetism of the mid-Tertiary Three Peaks Laccolith, Iron Axis Province, Southwest Utah. *Eos, Transactions of the American Geophysical Union* **87**(52).

RICHEY, J. E. 1932. Tertiary ring structures in Britain. *Transactions of the Geological Society of Glasgow* **19**, 42–140.

RICHEY, J. E. & THOMAS, H. H. 1930. *The geology of Ardnamurchan, North West Mull and Coll*. Memoirs of the Geological Survey. Scotland, Sheets 51 and 52. Edinburgh: HMSO.

RICHTER, C. & VAN DER PLUIJM, B. A. 1994. Separation of paramagnetic and ferromagnetic susceptibilities using low temperature magnetic susceptibilities and comparison with high field methods. *Physics of the Earth and Planetary Interiors* **82**, 113–23.

ROCHETTE, P. 1987. Magnetic susceptibility of the rock matrix related to magnetic fabric studies. *Journal of Structural Geology* **9**, 1015–20.

ROCHETTE, P., JACKSON, M. & AUBOURG, C. 1992. Rock magnetism and the interpretation of anisotropy of magnetic susceptibility. *Reviews of Geophysics* **30**(3), 209–26.

ROY, J. L. & PARK, J. K. 1974. The magnetization process of certain red beds: Vector analysis of chemical and thermal results, *Canadian Journal of Earth Sciences* **2**, 437–71.

SPARKS, R. S. J. 1988. Petrology and geochemistry of the Loch Ba ring-dyke, Mull N. W. Scotland ; an example

of the extreme differentiation of tholeiitic magmas. *Contributions to Mineralogy and Petrology* **100**, 446–61.

STEVENSON, C. T. E., OWENS, W. H. & HUTTON, D. W. H. 2007. Flow lobes in granite: the determination of magma flow direction in the Trawenagh Bay Granite, N. W. Ireland, using anisotropy of magnetic susceptibility. *Geological Society of America Bulletin* **119**, 1368–86.

STEVENSON, C. T. E., OWENS, W. H., HUTTON, D. H., HOOD, D. N. & MEIGHAN, I. G. 2007. Laccolithic, as opposed to cauldron subsidence, emplacement of the Eastern Mourne pluton, N. Ireland: evidence from anisotropy of magnetic susceptibility. *Journal of the Geological Society, London* **164**, 99–110.

TARLING, D. H. & HROUDA, F. 1993. *The magnetic anisotropy of rocks*. London: Chapman & Hall, 217 pp.

THOMPSON, R. N. 1982. Magmatism of the British Tertiary Volcanic Province. *Scottish Journal of Geology* **18**, 49–107.

TROLL, V. R., EMELEUS, C. H. & DONALDSON, C. H. 2000. Caldera formation in the Rum Igneous Complex, Scotland. *Bulletin of Volcanology* **62**, 301–17.

TROLL, V. R., DONALDSON, C. H. & EMELEUS, C. H. 2004. Pre-eruptive magma mixing in intra-caldera ash-flow deposits of the Rum Igneous Centre, Scotland. *Contributions to Mineralogy and Petrology* **147**, 722–39.

UYEDA, S., FULLER, M. D., BELSHE, J. C. & GIRDLER, R. W. 1963. Anisotropy of magnetic susceptibility of rocks and minerals. *Journal of Geophysical Research* **68**, 279–91.

WALKER, G. P. L. 1975. A new concept of the evolution of the British Tertiary intrusive centres. *Journal of the Geological Society, London* **131**, 121–41.

WILLSON, R. L., HALL, J. M. & DAGLEY, P. 1972. The British Tertiary igneous province: palaeomagnetism of the dyke swarm along the Sleat coast of Skye. *Geophysical Journal International* **68**, 317–23.

ZIJDERVELD, J. D. A. 1967. A. C. Demagnetization of rocks: Analysis of results. In *Methods in Paleomagnetism* (eds D. W. Collinson, K. M. Creer & S. K. Runcorn), pp. 254, 286. Amsterdam: Elsevier.